Received: 23 March 2023 | Revised: 25 July 2023 | Accepted: 16 August 2023

DOI: 10.1002/alz.13464

Alzheimer's & Dementia®
THE JOURNAL OF THE ALZHEIMER'S ASSOCIATION

RESEARCH ARTICLE

Anesthesia-induced hippocampal-cortical hyperactivity and tau hyperphosphorylation impair remote memory retrieval in Alzheimer's disease

Kai Chen[1] | **Riya Gupta**[2] | **Alejandro Martín-Ávila**[3] | **Meng Cui**[4] | **Zhongcong Xie**[5] | **Guang Yang**[1]

[1]Department of Anesthesiology, Columbia University Irving Medical Center, New York, New York, USA

[2]Barnard College of Columbia University, New York, New York, USA

[3]New York University School of Medicine, New York, New York, USA

[4]Department of Biology, Purdue University, West Lafayette, Indiana, USA

[5]Geriatric Anesthesia Research Unit, Department of Anesthesia, Critical Care and Pain Medicine, Massachusetts General Hospital and Harvard Medical School, Charlestown, Massachusetts, USA

Correspondence
Guang Yang, PhD, Associate Professor of Anesthesiological Sciences, Department of Anesthesiology, Columbia University Irving Medical Center, 650 W 168th ST, BB 306, New York, NY 10032, USA.
Email: gy2268@cumc.columbia.edu

Zhongcong Xie, MD, PhD, Professor of Anesthesia, Geriatric Anesthesia Research Unit, Department of Anesthesia, Critical Care and Pain Medicine, Massachusetts General Hospital and Harvard Medical School, 149 13th Street, Room 4310, Charlestown, MA 02129, USA.
Email: zxie@mgh.harvard.edu

Funding information
National Institutes of Health, Grant/Award Numbers: GM131765, AG041274, AG062509, NS118302; Alzheimer's Association, Grant/Award Number: AARFD-17-533584

Abstract

INTRODUCTION: Anesthesia often exacerbates memory recall difficulties in individuals with Alzheimer's disease (AD), but the underlying mechanisms remain unclear.

METHODS: We used in vivo Ca^{2+} imaging, viral-based circuit tracing, and chemogenetic approaches to investigate anesthesia-induced remote memory impairment in mouse models of presymptomatic AD.

RESULTS: Our study identified pyramidal neuron hyperactivity in the anterior cingulate cortex (ACC) as a significant contributor to anesthesia-induced remote memory impairment. This ACC hyperactivation arises from the disinhibition of local inhibitory circuits and increased excitatory inputs from the hippocampal CA1 region. Inhibiting hyperactivity in the CA1-ACC circuit improved memory recall after anesthesia. Moreover, anesthesia led to increased tau phosphorylation in the hippocampus, and inhibiting this hyperphosphorylation prevented ACC hyperactivity and subsequent memory impairment.

DISCUSSION: Hippocampal-cortical hyperactivity plays a role in anesthesia-induced remote memory impairment. Targeting tau hyperphosphorylation shows promise as a therapeutic strategy to mitigate anesthesia-induced neural network dysfunction and retrograde amnesia in AD.

KEYWORDS
Alzheimer's disease, anesthesia, anterior cingulate cortex, hippocampus, remote memory

1 | BACKGROUND

Episodic memory impairment is a prominent symptom of Alzheimer's disease (AD). Even in the presymptomatic stage, individuals with AD-related mutations face an elevated risk of difficulties retrieving recent or remote memories following stressful events like injury, infection, or anesthesia and surgery.[1–3] For example, patients with underlying dementia are more prone to developing postoperative delirium, and those who experience delirium exhibit an increased incidence of newly diagnosed dementia once the delirium episodes have subsided.[4] Studies in animals have suggested a potential link between exposure to anesthesia and the onset and progression of cognitive impairment and AD pathology.[5–8] However, the precise mechanism by which anesthesia detrimentally affects remote memory retrieval in presymptomatic AD is largely unknown.

Episodic memories are encoded within hippocampal and prefrontal circuits.[9] The acquisition of spatial memory, for instance, relies on the involvement of the hippocampus, with neuronal firing in the CA1 region playing a crucial role in the successful retrieval of recent memory.[10,11] Once memories are consolidated, the storage of remote or long-term memories appears to involve the anterior cingulate cortex (ACC), a subregion of the medial frontal cortex.[12] Previous studies demonstrated that the retrieval of remote memory led to an increased expression of activity-dependent genes and sustained neuronal activity in the ACC.[13–15] Conversely, both pharmacological and optogenetic inhibition of ACC impedes remote memory recall.[16,17]

Both the hippocampus and ACC are susceptible to neurological insults, and in the context of AD, the presence of intracellular aggregates of hyperphosphorylated tau, a microtubule-associated protein, can exacerbate their damage.[18–20] Increasing evidence suggests that anesthesia can significantly impact tau phosphorylation.[21] For example, repeated exposure of young or adult mice to sevoflurane, a commonly used inhalational anesthetic, induces tau hyperphosphorylation in the hippocampus, leading to cognitive impairment.[22–26] In aged mice, a single exposure to sevoflurane anesthesia results in a more than twofold increase in tau phosphorylation in the frontal cortex.[27] Furthermore, in patients, the incidence and severity of postoperative delirium have been linked to levels of total and phosphorylated tau in the serum,[28,29] while increased functional magnetic resonance imaging (fMRI) activity in the hippocampus of healthy older adults has shown a correlation with tau levels in cerebrospinal fluid (CSF).[30,31] Despite these associations, whether tau contributes to anesthesia-induced neural network dysfunction and remote memory deficits remains unclear.

In this study, we examined the impact of sevoflurane exposure on the recall of previously acquired memory in two mouse models of AD (5×FAD and APP/PS1). To explore the neuronal circuit mechanism underlying anesthesia-induced remote memory impairment, we employed a combination of in vivo two-photon Ca^{2+} imaging, viral-based circuit tracing, recombinase-mediated labeling, and chemogenetic techniques. Our results demonstrated that sevoflurane exposure led to a significant increase in pyramidal neuron activity in the ACC. This heightened activity was driven by the disinhibition of local inhibitory circuits and augmentation of long-range excitatory inputs originating from the hippocampal CA1 region. Furthermore, we showed that chemogenetic inhibition of CA1-ACC inputs rectified ACC neuronal hyperactivity and improved remote recall. Importantly, inhibiting tau hyperphosphorylation in the hippocampus prevented anesthesia-induced ACC hyperactivity and remote memory impairment. These findings in animals provide insights into anesthesia-induced remote memory deficits and highlight the therapeutic potential of targeting tau phosphorylation in AD-associated retrograde amnesia.

RESEARCH IN CONTEXT

1. **Systematic review**: The consolidation and retrieval of memory involve intricate interactions between the hippocampus and neocortex. In individuals with Alzheimer's disease (AD), this process is thought to be compromised. Animal studies have suggested that anesthesia can exacerbate difficulties in recalling previously acquired memories. However, the specific molecular and neural circuit mechanisms responsible for this effect remain poorly understood.
2. **Interpretation**: In our study, we used 5×FAD and APP/PS1 models of AD and observed that exposing presymptomatic mice to anesthesia resulted in a disruption of the recall of spatial memory they had previously acquired. Our findings indicate that this impairment of remote memory can be attributed to abnormal hyperactivation of the anterior cingulate cortex, triggered by anesthesia-induced tau hyperphosphorylation in the hippocampus.
3. **Future directions**: Future studies could employ other AD models, such as apolipoprotein E4 (*APOE4*), to determine whether anesthesia-induced memory impairment is mediated by similar mechanisms of neural network dysfunction. Additionally, assessing the therapeutic potential of tau inhibitors as interventions for memory impairment at various stages of disease progression would be valuable.

2 | METHODS

2.1 | Animals

Transgenic mouse strains, including 5×FAD (034840), APP/PS1 (004462), PV-T2A-Cre (012358), SST-IRES-Cre (013044), CRH-IRES-Cre (012704), and VIP-IRES-Cre (010908), were obtained from the Jackson Laboratory. *Thy1.2*-GCaMP6s line 1 mice were bred in-house.[32] Mice were group-housed in temperature-controlled rooms

with a 12-h light-dark cycle. They were randomly assigned to different treatment groups, and male and female mice aged 3 to 5 months were used in this study. All mice were kept at the Columbia University animal facility and handled in accordance with the National Institutes of Health (NIH) guidelines for animal care and use. The study procedures (protocol no. AABN7553) were approved by the Institutional Animal Care and Use Committee at Columbia University. No association was found between animals' sex and experimental results.

2.2 | Anesthesia and physiological measurements

Prolonged anesthesia duration is associated with an increased risk of postoperative complications.[33] To conceptually simulate such clinical scenarios, mice in the anesthesia group underwent 6 h of anesthesia, following established protocols from previous animal studies.[8,34] Specifically, the mice were placed in a transparent anesthesia chamber and administered 3% sevoflurane in 30% oxygen for 6 h. To prevent hypothermia,[35,36] the animals' body temperature was continuously monitored and regulated using a feedback-controlled system (World Precision Instruments Inc., Sarasota, FL, USA). The system automatically adjusted the heating pad positioned beneath the anesthesia chamber to maintain the mice's rectal temperature at approximately 37°C (Figure S1). After the mice recovered from anesthesia, they were returned to their home cages with ad libitum access to food and water. Mice in the control group remained in their home cages under room air conditions for the same 6-h duration.

Physiological measurements were performed on separate sets of animals following the same anesthesia procedure described above (Figure S1). Specifically, respiratory rates were determined by counting the number of thoracic breathing movements during a 30-s period and calculated as breaths per min. Heart rates were monitored independently using electrocardiogram signals. Artery blood gas analysis was performed using an iSTAT analyzer (Abbott Laboratories, Abbott Park, IL). Consistent with previous studies,[37] sevoflurane at 3% did not induce substantial changes in the mice's pH, pO_2, and pCO_2 values (Figure S1). No mortality was observed during the anesthesia procedure.

2.3 | Barnes maze

All behavioral experiments were conducted in a double-blind manner. The Barnes maze test is a well-established method for assessing spatial memory in rodents. In this study, we adopted a shortened protocol from a previous study[38] to conduct the Barnes maze test. The experiment was conducted on a circular platform with a diameter of 90 cm, featuring 19 evenly distributed holes around the edge and an escape hole. An escape cage (24 × 5 × 5 cm) was attached to the escape hole, providing a hiding place for the mice. Visuospatial cues were placed in the surrounding area to aid the mice in locating the escape cage, and an auditory cue (buzzer) was used as an environmental stimulus. Four training trials were conducted during the training day with 20-min intervals between each trial. The mice were placed in the center of the platform and given 5 s to acclimate before being allowed to explore the platform for 3 min to find the escape cage. If the mice could not locate the escape cage within the allotted time, the researcher guided them to it. The platform and escape cage were thoroughly cleaned using 75% alcohol between trials. Sixteen days after the training, spatial memory recall was assessed by testing the mice on the same platform for 3 min but with the escape cage removed. The recall performance was measured as the percentage of time the mice spent in the target quadrant. Behavioral data were recorded and analyzed using ANY-maze software (Stoelting, Wood Dale, IL).

2.4 | Open field

To assess locomotor function and anxiety-like behavior in mice, we used a standardized open field arena (40 × 40 cm), where the mice were observed and recorded for 10 min. Video tracking and behavioral data analysis were performed using the ANY-maze software. Several parameters, including total distance traveled and time spent in the central region of the arena, were quantified. The central region was defined as a square measuring 20 × 20 cm at the center of the testing field.

2.5 | Viruses and drugs

Recombinant AAV viral vectors were obtained from Addgene. Aliquoted AAVs were stored at −80°C, thawed on ice, and centrifuged before use. AAVs were stereotaxically injected into the targeted brain region using a picospritzer (34 KPa, 12 ms pulse width, 0.3 to 0.4 Hz). The injection speed was ∼10 to 15 min per 0.1 μL, allowing an additional 10 to 15 min for spreading at the injection site before withdrawing the glass micropipette. The coordinates for viral injections were as follows: ACC (anterior-posterior (AP) 0.8 mm, medial-lateral (ML) 0.3 mm, and subpial (SP) 0.6 mm), mediodorsal thalamus (MDT) (AP −1.60 mm, ML 0.6 mm, SP 2.8 mm), dorsal hippocampal CA1 (AP −2.0 mm, ML 1.5 mm, SP 1.5 mm). Viruses were injected into the ACC, MDT, or CA1 at least 2 weeks before the experiments. The titer (genome copies per mL, gc mL^{-1}) and stock number for each vector were as follows: AAV1-Syn-FLEx-GCaMP6s (>1 × 10^{13} gc mL^{-1}; Stock No. 100845), AAVrg-CaMKIIα-mCherry (7 × 10^{12}; 114469), AAV1-hSyn-Cre (7 × 10^{12}; 105553), AAV1-CaMKII-Cre (1 × 10^{13}; 105558), AAV9-hSyn-FLEx-axon-GCaMP6s (1 × 10^{13}; 112010), AAV8-CaMKIIα-hM3Dq-mCherry (3 × 10^{12}; 50476), AAV9-hSyn-DIO-hM_4Di-mCherry (1 × 10^{13}; 44362), AAV9-hSyn-DIO-hM_3Dq-mCherry (1 × 10^{13}; 44361), and AAV2/1-FLEx-tdTomato (1 × 10^{13}; 28306).

To reduce neuronal hyperactivity, mice were intraperitoneally administered a low dose of clonazepam (0.05 mg/kg) or vehicle (saline). To inhibit tau phosphorylation in the hippocampus,[39] 0.15 μL of LiCl (100 mM, L7026, Sigma) or vehicle was bilaterally infused into the CA1 regions.

2.6 | Surgical preparation for imaging awake, head-restrained mice

The surgical procedure for preparing a cranial window to image the mouse cortex was described previously.[40] Specifically, mice were deeply anesthetized with 100 mg kg^{-1} ketamine and 15 mg kg^{-1} xylazine. Following disinfection and scalp removal, a head plate (CF-10, Narishige) was attached to the surface of the mouse's skull using glue and dental acrylic. The ACC was identified using stereotaxic coordinates (AP, 0.8 mm; ML, 0.3 mm), and a cranial window was created over the ACC while ensuring the preservation of the intact dura. The cranial window was then covered with a silicon elastomer, and the mice were given at least 24 h to recover.

To prepare the hippocampal imaging window, a modified protocol was used based on previous reports.[41,42] After head plate mounting, a craniotomy was performed in the parietal bone, specifically over the dorsal hippocampus, using a microdrill. The bone flap was carefully removed, and debris or blood was cleaned. The meninges and cortical matter were removed using a blunt needle connected to a vacuum pump. Artificial CSF (ACSF) was applied throughout the tissue removal process to prevent dehydration. A 1.5-mm-long cannula was slowly inserted into the cortex until the glass coverslip at the bottom made contact with the hippocampus. Once the cannula was inserted, the skull was cleaned, and a mixture of adhesive cement was applied to the rim of the cannula and the skull. It was then left to dry and harden for 20 min. Finally, a removable adhesive film was used to cover the imaging window, preventing debris from entering the cannula. Following the surgery, mice were monitored daily and received subcutaneous administration of anti-inflammatory drugs (Meloxicam, 1 mg/kg) for 2 days. Mice were used for in vivo imaging 1 to 2 weeks after the window implantation. Before the imaging day, the mice underwent habituation to the imaging platform through two sessions, each lasting 10 min, to minimize head fixation stress.

2.7 | In vivo Ca^{2+} imaging and data analysis

Thy1-GCaMP6s mice were used for Ca^{2+} imaging of pyramidal neurons in the ACC. For Ca^{2+} imaging of inhibitory interneurons, 0.2 μL of AAV2/1-hSyn-FLEx-GCaMP6s was injected into the ACC of *Crh*$^{IRES\text{-}Cre}$, *Sst*$^{IRES\text{-}Cre}$, *Pvalb*$^{T2A\text{-}Cre}$, and *Vip*$^{IRES\text{-}Cre}$ mice. For imaging Ca^{2+} in MDT-ACC glutamatergic axons, a 0.2-μL mixture (volume ratio 1:1) of AAV1-CaMKII-Cre and AAV9-hSyn-FLEx-axon-GCaMP6s was injected into the MDT. Similarly, to image Ca^{2+} in CA1-ACC glutamatergic axons, a 0.2-μL mixture (volume ratio 1:1) of AAV1-CaMKII-Cre and AAV9-hSyn-FLEx-axon-GCaMP6s was injected into the CA1. To image Ca^{2+} activity in CA1-ACC projection neurons, 0.15 μL of AAVrg-pkg-Cre was injected into the ACC, while 0.2 μL of AAV1-Syn-FLEx-GCaMP6s was injected into the CA1.

Each animal underwent one Ca^{2+} imaging session 24 h after exposure to sevoflurane or air. Before imaging, the silicon elastomer or adhesive film was removed, and the cranial window was cleaned twice using ACSF. Subsequently, the mice were positioned on the stage of a Scientifica two-photon microscope equipped with a Ti: Sapphire laser (Vision S, Coherent) tuned to 920 nm. For Ca^{2+} imaging in the ACC, images were collected at depths of 700 to 900 μm below the pial surface to detect somas of L5 pyramidal neurons, 200 to 500 μm for interneurons, and ~150 μm for long-range projecting axons. For Ca^{2+} imaging in the hippocampal CA1, images were collected at depths of 100 to 600 μm below the glass window. Time-lapse imaging was performed in two fields of view to capture 50 to 100 somas or axons per animal for analysis. All images were acquired using a frame rate of 1.07 Hz and an image size of 512 × 512 pixels, using a 20× objective (1.0 N.A.) immersed in ACSF with a digital zoom of 1.5 or 2× for cortical neurons and 4× for axons. Image acquisition was performed using ScanImage software (version 5.4; Vidrio Technologies).

The Ca^{2+} imaging data were analyzed using NIH ImageJ software, following the method described previously.[43] In brief, the raw images were registered and motion-corrected using the TurboReg plugin for ImageJ. Regions of interest (ROIs) were manually selected to correspond to visually identifiable axons and somas. Background fluorescence was subtracted for each ROI, and the pixel values within the ROI were averaged to generate a time-series fluorescence trace, which was represented as $\Delta F/F_0 = (F - F_0)/F_0$, where F_0 is the baseline fluorescence averaged over a 6-s period corresponding to the lowest fluorescence signal during the recording session. The Ca^{2+} activity was quantified by averaging $\Delta F/F_0$ over a 3- to 10-min recording session. Neurons exhibiting a Ca^{2+} transient frequency >5 min^{-1} were classified as hyperactive, while those with a frequency <1 min^{-1} were classified as inactive. Neurons displaying frequencies within this range were classified as normal.

2.8 | Chemogenetic manipulation

To inhibit or activate ACC excitatory neurons, 0.2 μL of inhibitory or excitatory DREADD (AAV8-CaMKIIα-hM$_4$Di-mCherry or AAV8-CaMKIIα-hM$_3$Dq-mCherry) or control vectors (AAV8-CaMKIIα-mCherry) were bilaterally injected into the ACC of 5×FAD mice. To inhibit VIP interneurons, 0.2 μL of inhibitory DREADD (AAV9-hSyn-DIO-hM$_4$Di-mCherry) or control vectors (AAV9-hSyn-DIO-mCherry) were bilaterally injected into the ACC of *Vip*$^{IRES\text{-}Cre}$; 5×FAD mice. To inhibit CA1-ACC projection neurons, 0.2 μL of AAV9-hSyn-DIO-hM$_4$Di-mCherry was bilaterally injected into the CA1 regions, while 0.2 μL of AAVrg-pkg-Cre was bilaterally injected into the ACC of 5×FAD mice. For mice expressing hM$_3$Dq or hM$_4$Di receptors, 2 mg/kg CNO (C0832; Sigma-Aldrich) was administered via intraperitoneal injection 30 min before imaging or behavioral experiments.

2.9 | Cell-type specific circuit dissection

For retrograde labeling of excitatory neurons projecting to the ACC, 0.25 μL of AAVrg-CaMKIIα-mCherry was unilaterally injected into the

ACC of C57BL/6 mice. To label the ACC neurons receiving monosynaptic projections from the CA1, 0.2 μL of AAV1-hSyn-Cre was injected into the CA1, and 0.15 μL of AAV2/1-hSyn-tdTomato was injected into the ipsilateral ACC of C57BL/6 mice.

2.10 | Immunohistology and data analysis

Mice were deeply anesthetized and then perfused with 30 mL phosphate-buffered solution (PBS), followed by 20 mL of 4% paraformaldehyde (PFA). The brain was collected and further fixed in PFA for 24 h. After fixation, the brain tissues were dehydrated with 30% sucrose for 3 days. The brain was then sectioned into 60-μm coronal slices using a Leica vibratome (VT-1000S). The brain slices were washed twice in PBS for 10 min each, then blocked with a mixture of donkey serum and 1% Triton X-100 at room temperature for 2 h. Subsequently, the slices were incubated with primary antibodies (anti-CaMKIIα, Cell Signaling Technology, 50049; anti-GABA, Sigma-Aldrich, A2052; anti-parvalbumin, Abcam, ab11427; anti-somatostatin, Abcam, ab30788; anti-vasoactive intestinal polypeptide, Cell Signaling Technology, 63269; anti-c-Fos, Cell Signaling Technology, 2250; anti-phospho-tau (AT8), Invitrogen, MN1020B) at 4°C for ~48 h. After the primary antibody incubation, the slices were washed three times with PBS to remove any remaining primary antibodies and then incubated with secondary antibodies (anti-rabbit Alexa Fluor 488; anti-mouse Alexa Fluor 488; anti-mouse Alexa Fluor 564) for 2 h at room temperature. Following another round of washing, the slices were mounted with a mounting medium containing DAPI and covered with coverslips.

Confocal imaging was performed using a Nikon Ti laser scanning confocal system with a 20× objective. Images captured with different fluorescent channels were merged using ImageJ software, and the number of cells was subsequently calculated using the same software.

2.11 | Statistical analysis

Statistical analyses were performed using Prism 7.0 (GraphPad Software, Inc). Summary data were presented as mean ± SEM. Sample sizes were determined based on our previous studies [44,45] to ensure adequate statistical power while minimizing the number of animals used, in accordance with ethical guidelines. No animals that were successfully measured were excluded from the analysis. Tests for differences between two populations were performed using Student's *t* test or nonparametric Mann-Whitney U-test. Multiple-group comparisons were performed using one-way ANOVA followed by Bonferroni's *post hoc* tests. All comparisons were two-tailed. The significance level was set at $p < .05$. All statistical details of the experiments can be found in the figure legends.

3 | RESULTS

3.1 | Sevoflurane impairs remote memory retrieval in presymptomatic AD mice

To investigate the potential impact of anesthesia on the retrieval of previously acquired memory, we conducted a study using wild-type (WT) and presymptomatic AD transgenic mice, specifically 3-month-old 5×FAD mice and 5-month-old APP/PS1 mice (Figure 1A). Mice were trained in a Barnes maze task to assess spatial learning and memory (Figure 1B). This task involved identifying a dark, enclosed escape cage in an open environment using visuospatial cues surrounding the maze. Both WT and presymptomatic AD mice showed successful acquisition of spatial memory during the training phase (day 0), as evidenced by a progressive decrease in latency to identify the escape cage across four training trials (Figure 1C). To evaluate remote memory, we delayed the recall test by 16 days. On the day preceding the recall test (day 15), the mice were exposed to 3% sevoflurane or air for 6 h. We found that WT mice treated with sevoflurane displayed a comparable amount of time spent in the target quadrant (where the escape cage is located) during the recall test compared to WT mice treated with air (Figure 1D and Figure S2). In contrast, 5×FAD mice in the sevoflurane group spent significantly less time in the target quadrant than those in the air group (Figure 1D), indicating a decline in remote recall following recent sevoflurane exposure. Similarly, 5-month-old APP/PS1 mice in the sevoflurane group also exhibited impaired memory recall in the Barnes maze test compared to those in the air group (Figure 1D). These results indicate that exposure of presymptomatic AD mice to sevoflurane impairs the retrieval of remote memory they had previously acquired.

We further verified that sevoflurane had no significant impact on the animals' locomotor activity (Figure 1E and 1F). The data analysis from the open field test revealed no significant difference in the total distance traveled between the sevoflurane and air groups. Additionally, mice in the sevoflurane group displayed no signs of anxiety-like behavior, as indicated by their comparable amount of time spent in the center of the open field arena (Figure 1F).

3.2 | ACC hyperactivation following sevoflurane anesthesia

The ACC plays a critical role in contextual information processing and memory retrieval.[16] To examine the impact of sevoflurane on cortical network activity, we conducted immunostaining for c-Fos, a marker of neuronal activity. Remarkably, we observed that 1 day after sevoflurane exposure, the number of c-Fos$^+$ cells in the ACC of 5×FAD mice was approximately three times higher compared to the air-exposed group (Figure S3).

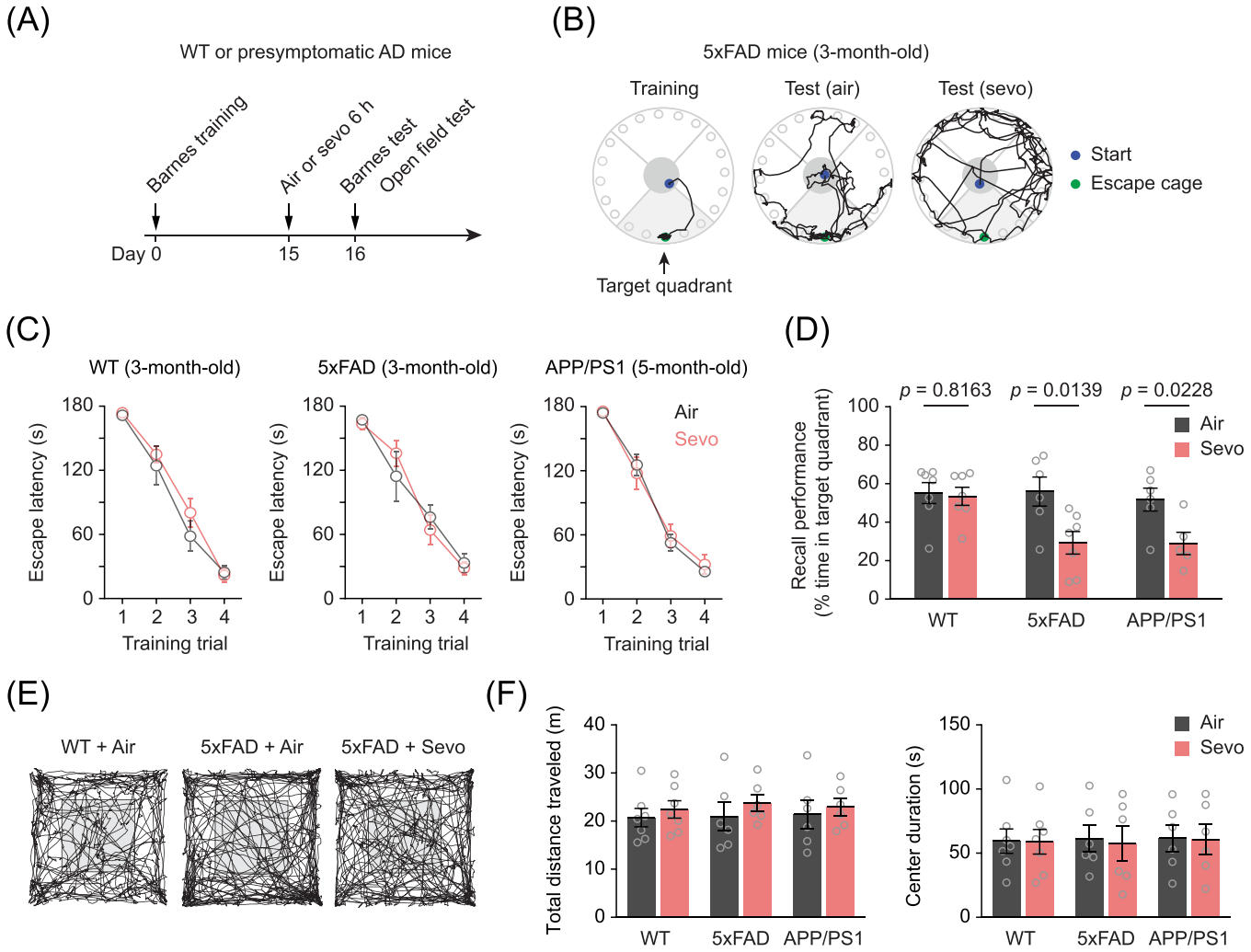

FIGURE 1 Sevoflurane exposure impairs remote memory retrieval in presymptomatic AD mice. (A) Experimental timeline. (B) Representative navigation path during the Barnes maze training (left) and recall test for 3-month-old 5×FAD mice treated with air (middle) or sevoflurane (right). (C) Latency to locate the escape cage across four trials during the training day in 3-month-old WT mice, 3-month-old 5×FAD mice, and 5-month-old APP/PS1 mice. (D) Recall performance during test, assessed by time spent in target quadrant, for WT mice ($n = 7$ mice per group; unpaired t test, $t_{12} = 0.2349$, $p = .8163$), 5×FAD mice ($n = 6, 7$ mice; unpaired t test, $t_{11} = 2.834$, $p = .0139$), and APP/PS1 mice ($n = 6, 5$ mice; unpaired t test, $t_9 = 2.714$, $p = .0228$). (E) Representative trajectory plots of mice exploring an open field arena. (F) Total distance traveled and time spent in center region of open field arena. Summary data are presented as mean ± SEM. Each dot represents data from a single animal (D, F).

To investigate cell type-specific activity changes, we performed in vivo Ca^{2+} imaging in the ACC of 5×FAD mice crossed with *Thy1.2*-GCaMP6 mice, which express the genetically encoded Ca^{2+} indicator GCaMP6s specifically in layer 5 (L5) pyramidal neurons (Figure 2A). Using a cranial window, we visualized GCaMP6s-expressing pyramidal neurons in the ACC, located at depths of 700 to 900 μm below the pial surface and 400 to 600 μm away from the midline (Figure 2B). Following 6-h exposure to sevoflurane, we observed an approximately threefold increase in Ca^{2+} activity in the somas of ACC pyramidal neurons in 5×FAD mice during a resting state. This increase was evident in measurements of the area under the curve (AUC), frequency, and peak amplitude of Ca^{2+} transients compared to air-treated controls (Figure 2C). Furthermore, sevoflurane-exposed 5×FAD mice exhibited a higher percentage of hyperactive ACC pyramidal neurons compared to air-exposed mice (14.3% vs 4.7%) (Figure 2D), which is consistent with the observed increase in c-Fos$^+$ cells. Importantly, the level of hyperactivity in ACC pyramidal neurons in 5×FAD mice correlated with the spatial memory impairment observed in the Barnes maze test (Figure 2E). Similarly, in 5-month-old APP/PS1 mice, we observed elevated somatic Ca^{2+} activity in ACC pyramidal neurons 24 h after sevoflurane exposure compared to air-exposed mice (Figure 2F,G). This activity increase also correlated with recall performance (Figure 2H). In contrast, the same sevoflurane exposure had no significant effects on ACC neuronal Ca^{2+} activity in WT mice (Figure S4). These results indicate that sevoflurane anesthesia induces hyperactivation of pyramidal neurons in the ACC of presymptomatic AD mice.

To examine the role of ACC hyperactivation in remote memory impairment in presymptomatic AD mice, we used a chemogenetic approach to specifically modulate ACC neuronal activity. We used Cre-dependent adeno-associated viruses (AAV) to express either an

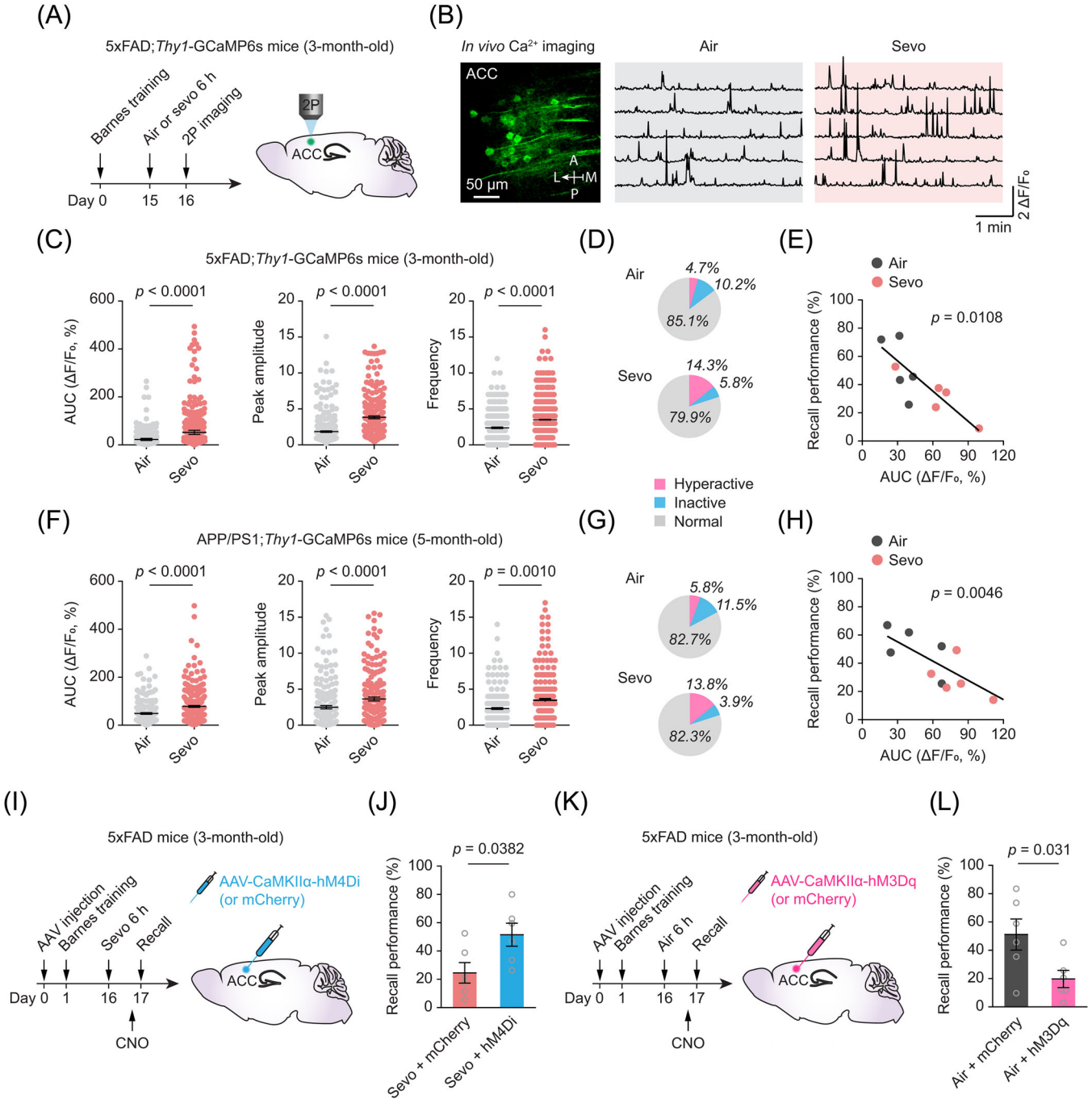

FIGURE 2 Sevoflurane exposure causes pyramidal neuron hyperactivity in ACC of presymptomatic AD mice. (A) Experimental timeline for Barnes maze training, sevoflurane exposure, and in vivo two-photon (2P) Ca^{2+} imaging in ACC of 5×FAD; *Thy1*-GCaMP6s mice. (B) Representative image of L5 pyramidal neurons expressing GCaMP6s (left) and Ca^{2+} traces (right). (C) Quantification of area under the curve (AUC), peak amplitude, and frequency of Ca^{2+} transients in 5×FAD mice treated with air or sevoflurane ($n = 245, 353$ cells from four to five mice per group, unpaired *t* test; AUC: $t_{596} = 3.64$, $p < .0001$; amplitude, $t_{596} = 2.383$, $p < .0001$; frequency, $t_{596} = 2.99$, $p < .0001$). (D) Percentage of hyperactive neurons following air or sevoflurane exposure. (E) Recall performance correlates with pyramidal neuronal Ca^{2+} activity in ACC of 5×FAD mice (Pearson correlation, $r^2 = 0.65$, $p = .0108$). (F–H) Similar to (C)–(E), but for APP/PS1 mice ($n = 199, 309$ cells from four to five mice per group, unpaired *t* test; AUC: $t_{506} = 5.459$, $p < .0001$; amplitude, $t_{506} = 5.822$, $p < .0001$; frequency, $t_{506} = 2.908$, $p = .0010$; Pearson correlation, $r^2 = 0.57$, $p = .0046$). (I) Experimental design for chemogenetic inhibition of excitatory neurons in ACC 30 min prior to recall test. 5×FAD mice were previously trained in the Barnes maze and exposed to sevoflurane for 6 h 1 day before the recall test. (J) Inhibition of ACC neuronal hyperactivity improves recall performance in 5×FAD mice with recent sevoflurane exposure ($n = 6$ mice per group, unpaired *t* test, $t_{10} = 2.475$, $p = .0382$). (K) Experimental design for chemogenetic activation of excitatory neurons in ACC prior to recall test. 5×FAD mice were previously trained in Barnes maze and exposed to room air. (L) Chemogenetic activation of ACC excitatory neurons impairs remote memory recall in 5×FAD mice without sevoflurane exposure ($n = 6$ mice per group, unpaired *t* test, $t_{10} = 2.508$, $p = .031$). Summary data are presented as mean ± SEM. Each dot represents data from a single cell (C, F) or animal (E, H, J, L).

inhibitory DREADD variant, hM_4Di, or mCherry (control), under the control of a CaMKIIα promoter. This strategy ensured selective DREADD expression in excitatory neurons (Figure 2I and Figure S5). Activation of hM_4Di receptors by the ligand clozapine N-oxide (CNO) led to the opening of G-protein inwardly rectifying potassium channels, resulting in membrane hyperpolarization and reduced neuronal firing.[46] Two weeks after the Barnes maze training, 5×FAD mice expressing hM_4Di in ACC excitatory neurons were exposed to sevoflurane for 6 h. The subsequent day, mice were administered CNO 30 min prior to the memory recall test. We found that inhibition of anesthesia-induced ACC neuronal hyperactivity substantially increased the time spent by mice in the target quadrant (Figure 2J), suggesting an improvement in memory retrieval.

To further examine the causal relationship between ACC hyperactivation and remote memory impairment in presymptomatic AD, we used an excitatory DREADD variant, hM_3Dq, to enhance neuronal activity in the ACC of 5×FAD mice exposed to air (without sevoflurane) (Figure 2K). After viral infection and Barnes maze training, mice received CNO administration 30 min prior to the recall test. We found that direct activation of ACC excitatory neurons with hM_3Dq significantly reduced the time spent by mice in the target quartet, indicating impaired memory recall (Figure 2L). These results collectively demonstrate the critical role of ACC hyperactivation in remote memory impairment in presymptomatic AD mice.

3.3 | Enhanced vasoactive intestinal peptide interneuron activity in ACC

Cortical pyramidal neurons receive regulatory input from local inhibitory circuits, which consist of various subtypes of interneurons, including corticotropin-releasing hormone (CRH), somatostatin (SST), parvalbumin (PV), and vasoactive intestinal peptide (VIP)-expressing interneurons (Figure 3A). To better understand the impact of sevoflurane on ACC circuits, we used Cre-dependent AAV to express GCaMP6s in *Crh*$^{IRES\text{-}Cre}$, *Sst*$^{IRES\text{-}Cre}$, *Pvalb*$^{T2A\text{-}Cre}$, and *Vip*$^{IRES\text{-}Cre}$ mice crossed with 5×FAD and then imaged Ca^{2+} activity of interneurons 24 h after sevoflurane exposure (Figure 3B,C). Previous studies suggested that CRH-expressing neurons are involved in stress response and behavior, such as anxiety and social withdrawal.[47,48] Our results showed that sevoflurane exposure had no significant effect on the Ca^{2+} activity of CRH-expressing neurons (Figure 3D, $p = .7174$), which aligns with our behavioral data showing that these mice did not exhibit anxiety-like behavior in the open field test after sevoflurane exposure (Figure 1F).

SST and PV interneurons directly inhibit cortical pyramidal neurons, while VIP interneurons can indirectly disinhibit them.[49] One day after sevoflurane anesthesia, SST interneurons showed no significant changes in somatic Ca^{2+} activity (Figure 3E, $p = .8403$). PV interneurons, on the other hand, displayed a trend toward decreased Ca^{2+} activity, although it did not reach statistical significance (Figure 3F, $p = .0547$). Notably, VIP interneurons exhibited a substantial increase in Ca^{2+} activity 24 h after sevoflurane exposure (Figure 3G, $p < .0001$), suggesting a potential role for these cells in sevoflurane-induced ACC disinhibition in presymptomatic AD mice.

To confirm the involvement of VIP interneurons in ACC pyramidal neuron hyperactivation and remote memory recall impairment, we chemogenetically reduced VIP activity in vivo. Specifically, we bilaterally injected a Cre-dependent AAV encoding hM_4Di into the ACC of *Vip*$^{IRES\text{-}Cre}$; 5×FAD; *Thy1*-GCaMP6s mice (Figure 3H,I). Following Barnes maze training and sevoflurane exposure, we observed that inhibition of VIP interneurons significantly reduced the hyperactivity of pyramidal neurons, bringing their activity levels comparable to those in air-treated mice (Figure 3J). Furthermore, when mice were administered CNO 30 min prior to testing for Barnes maze recall, we found that CNO treatment was sufficient to reverse the remote memory impairment induced by sevoflurane exposure (Figure 3K).

3.4 | Elevated excitatory inputs from CA1 to ACC

To investigate the mechanisms underlying the increased activity of VIP and pyramidal neurons in the ACC following sevoflurane exposure, we focused on identifying the source of excitatory input to the ACC. As a cognitive and affective processing hub, the ACC receives extensive projections from various brain regions.[50] To determine the origin of excitatory input, we injected a retrograde transducing AAV (AAVrg) carrying mCherry under the control of a CaMKIIα promoter into the ACC of C57BL/6 mice. Three weeks after viral infection, we observed significant retrograde labeling of ACC-projecting neurons ($mCherry^+$) in several brain regions, including the MDT, dorsal and ventral hippocampus (dCA1 and vCA1), orbitofrontal cortex, basolateral amygdala, lateral hypothalamus, and median raphe nucleus (Figure S6). Among these brain regions, the MDT and CA1 exhibited the highest number of $mCherry^+$ cells.

To test the potential involvement of projections from the MDT in activating the ACC after sevoflurane anesthesia,[51] we examined the activity of MDT axonal terminals in the ACC. To do this, we selectively expressed axon-targeted GCaMP6s[52] in the excitatory neurons of the MDT in 3-month-old 5×FAD mice and performed axonal Ca^{2+} imaging in the ACC 1 day after sevoflurane exposure (Figure 4A). Immunostaining of brain slices revealed that MDT axonal terminals were concentrated in layers 1 and 5 of the ACC (Figure S7), consistent with previous reports.[53] Surprisingly, we did not observe significant changes in the levels of Ca^{2+} activity in MDT terminals following the 6-h sevoflurane exposure (Figure 4B), suggesting a minimal role of MDT inputs in driving ACC hyperactivation.

Previous studies established the crucial role of the hippocampus in encoding and retrieving spatial memory,[10] and it is known to be particularly vulnerable to damage during the early stages of AD pathogenesis.[54] Using the same method as that described earlier, we expressed axonal GCaMP6s in the CA1 pyramidal neurons of 3-month-old 5×FAD mice (Figure 4C). After viral expression, the presence of CA1 terminals was primarily observed in layers 1, 2/3, and 6 of the ACC (Figure S7). One day after sevoflurane exposure, we observed a significant increase in CA1 axonal Ca^{2+} levels in the ACC of 5×FAD

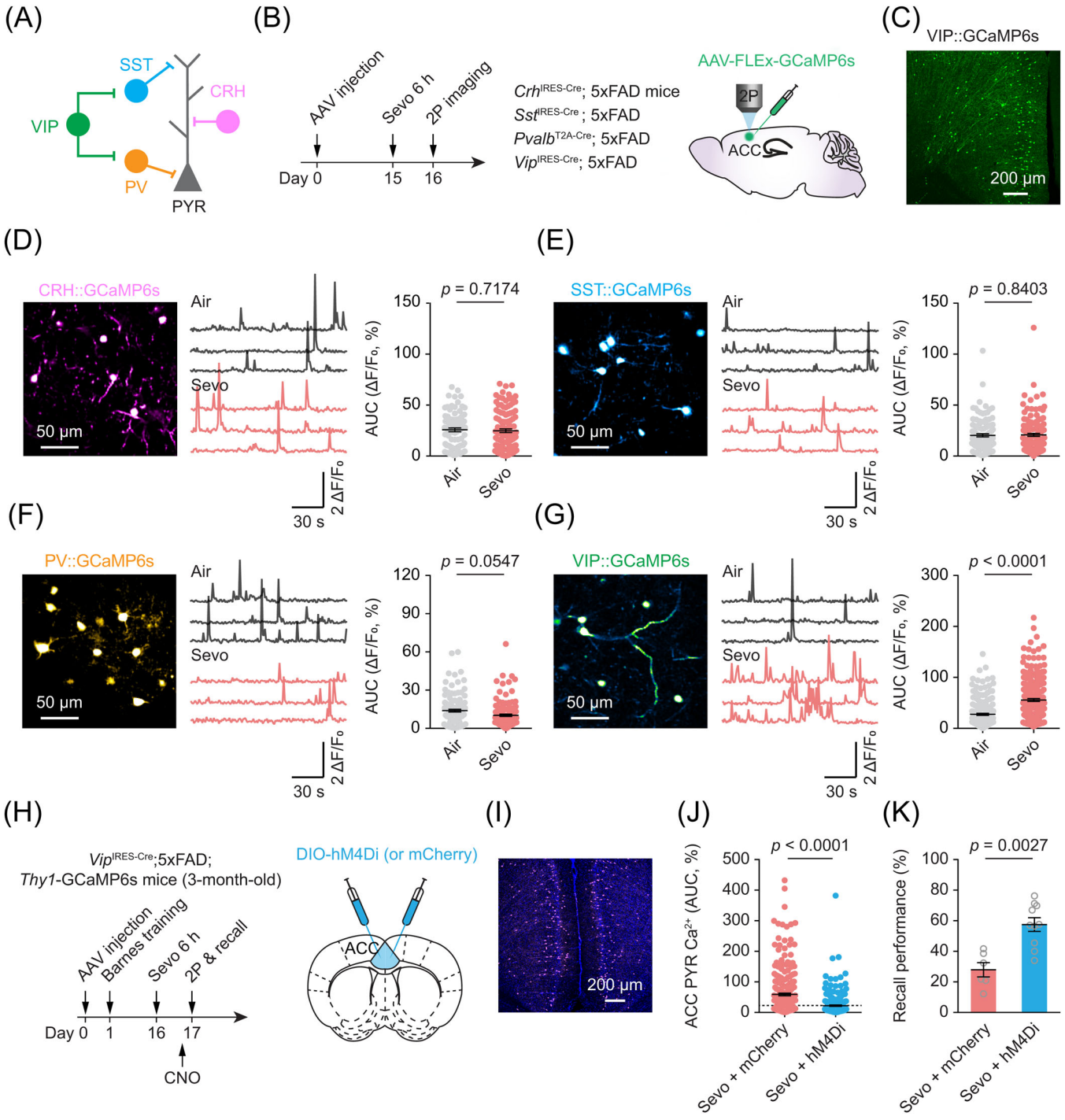

FIGURE 3 Sevoflurane exposure induces VIP cell hyperactivity in ACC of presymptomatic AD mice. (A) Schematic of ACC local circuitry. PYR, pyramidal neurons; PV, parvalbumin-expressing interneurons; SST, somatostatin-expressing interneurons; CRH, corticotropin-releasing hormone neurons; VIP, vasoactive intestinal peptide-expressing interneurons. (B) Experimental timeline and design for cell-type-specific expression of GCaMP6s in ACC of 5×FAD mice. (C) Example image of ACC showing VIP interneurons expressing GCaMP6s. (D) Representative image (left), Ca^{2+} traces (middle), and quantification of average Ca^{2+} activity in CRH neurons ($n = 82, 117$ cells from three mice per group, unpaired t test, $t_{197} = 0.3625$, $p = .7174$). (E–G) Similar to (D), but for SST (E, $n = 109, 132$ cells from three mice per group, unpaired t test, $t_{239} = 0.2017$, $p = .8403$), PV (F, $n = 119, 132$ cells from three mice per group, unpaired t test, $t_{249} = 1.93$, $p = .0547$), and VIP interneurons (G, $n = 193, 240$ cells from five mice per group, unpaired t test, $t_{431} = 8.129$, $p < .0001$). (H) Experimental timeline for chemogenetic inhibition of VIP cells in ACC of 5×FAD; *Thy1*-GCaMP6s mice with recent exposure to sevoflurane. (I) Representative image of ACC region showing $mCherry^+$ neurons. (J) Pyramidal neuron Ca^{2+} activity in ACC of 5×FAD mice expressing hM_4Di in VIP cells ($n = 280, 257$ cells from four mice per group, unpaired t test, $t_{535} = 7.453$, $p < .0001$). The dashed line indicates the Ca^{2+} level in 5×FAD mice with air exposure. (K) Inhibition of VIP cell hyperactivity improves recall performance in sevoflurane-exposed 5×FAD mice ($n = 6, 10$ mice, unpaired t test, $t_{14} = 4.332$, $p = .0027$). Summary data are presented as mean ± SEM. Each dot represents data from a single cell (D–G, J) or animal (K).

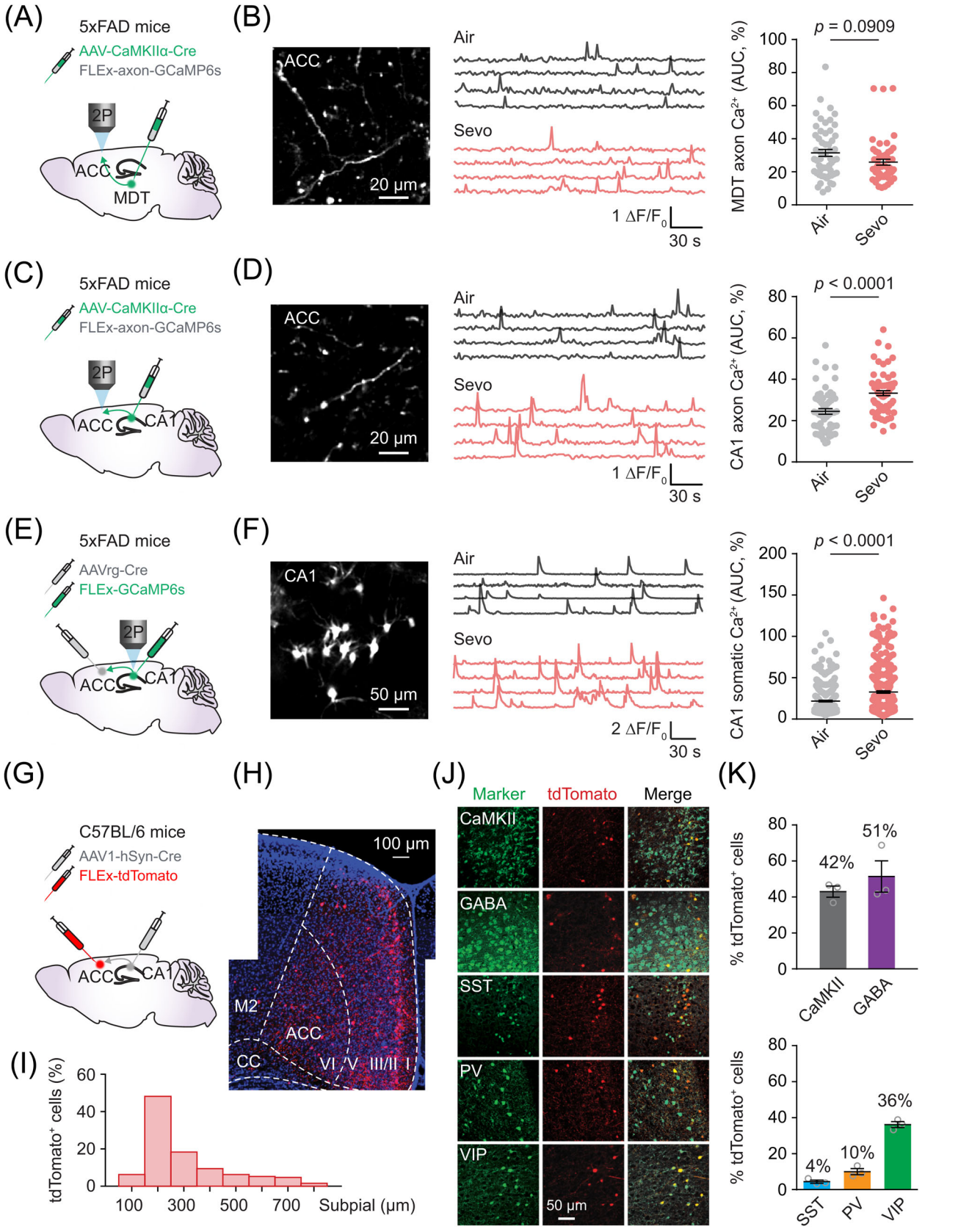

FIGURE 4 Sevoflurane exposure induces increased excitatory inputs from hippocampus to ACC. (A) Experimental design for imaging MDT→ACC axonal terminals in ACC. (B) Representative two-photon image (left), Ca^{2+} traces (middle), and quantification of axonal Ca^{2+} activity in 3-month-old 5×FAD mice with recent exposure to air or sevoflurane ($n = 82$, 117 axons from four mice per group, Mann–Whitney test,

mice compared to air-exposed mice (Figure 4D). To further confirm that CA1 neurons projecting to the ACC were indeed hyperactive following sevoflurane anesthesia, we injected AAVrg-Cre into the ACC and simultaneously injected FLEx-GCaMP6s into the hippocampal CA1 (Figure 4E). This injection strategy allowed for the selective expression of GCaMP6s in CA1 pyramidal neurons that project to the ACC. In vivo Ca^{2+} imaging in the dorsal hippocampal CA1 of 5×FAD mice revealed a substantial increase in somatic Ca^{2+} levels in these ACC-projecting neurons 24 h after sevoflurane exposure (Figure 4F). Collectively, these in vivo Ca^{2+} recordings demonstrate that sevoflurane induces a potent activation of CA1-ACC circuits in 5×FAD mice.

Using an AAV-mediated anterograde transsynaptic tracing strategy, we characterized the connectivity within the CA1-ACC circuit in C57BL/6 mice. Specifically, we injected AAV1-hSyn-Cre into the CA1 region and Cre-dependent tdTomato into the ACC (Figure 4G). Leveraging the anterograde transsynaptic spread properties of AAV1,[55] this approach allowed for the selective expression of tdTomato in ACC neurons that receive monosynaptic projections from CA1. After 3 weeks of viral infection, we visualized tdTomato$^+$ cells in brain sections using confocal imaging (Figure 4H) and found that they were distributed across all layers of the ACC, with a majority located in layer 2/3 (Figure 4I). Among the tdTomato$^+$ cells, approximately 42% were CaMKIIα^+, and 51% were GABA$^+$ (Figure 4J,K), indicating the presence of both glutamatergic and GABAergic neurons in the ACC forming synaptic connections with CA1 projection neurons. Notably, a significant fraction (36%) of tdTomato$^+$ cells were positive for VIP (Figure 4J,K). These findings indicate that CA1 neurons primarily project to pyramidal neurons and VIP interneurons in the ACC.

3.5 | Targeting CA1-ACC circuits to protect remote memory

To investigate whether targeting CA1-ACC circuits could protect against remote recall impairment following anesthesia exposure, we used an inhibitory DREADD approach to decrease the activity of CA1-ACC projection neurons in vivo. Specifically, we injected AAVrg-Cre into the ACC of 5×FAD; *Thy1*-GCaMP6s mice and simultaneously injected Cre-dependent hM_4Di or mCherry (control) into the CA1 (Figure 5A, Figure S8). After training the mice on the Barnes maze and administering sevoflurane anesthesia to mice expressing hM_4Di or mCherry in CA1-ACC projection neurons, we administered CNO and performed Ca^{2+} imaging in ACC pyramidal neurons 30 min later. As expected, a single injection of CNO effectively inhibited CA1 neurons, as evidenced by the reduction of c-Fos$^+$ cells (Figure S8). Subsequently, we observed a marked reduction in Ca^{2+} activity in ACC pyramidal neurons, bringing their activity levels to a range comparable to those observed in 5×FAD mice without sevoflurane exposure (Figure 5B). Furthermore, the sevoflurane-induced impairment of remote memory in 5×FAD mice was significantly reversed upon the inactivation of CA1 neurons by CNO (Figure 5C). As a control, the injection of CNO in 5×FAD mice expressing mCherry (without hM_4Di) had no observable effects on ACC neuronal activity and remote recall.

In a separate experiment, we tested whether chemogenetic activation of CA1-ACC projection neurons in presymptomatic AD mice could replicate the negative impact of sevoflurane on neuronal activity in the ACC and remote recall in mice. For this purpose, we injected AAVrg-Cre and Cre-dependent hM_3Dq into the ACC and CA1 of 3-month-old 5×FAD mice, respectively (Figure 5D). Two weeks after Barnes maze training, these mice received a single dose of CNO after air exposure (without sevoflurane). Immunostaining of c-Fos confirmed the successful activation of CA1 neurons (Figure S8). As a result of CA1 neuronal activation, we observed a threefold increase in Ca^{2+} activity in ACC pyramidal neurons (Figure 5E). Subsequently, when these mice were subjected to the Barnes maze test for spatial memory recall, we noted a substantial decline in their spatial memory performance (Figure 5F). These findings indicate that excessive activation of CA1 pyramidal neurons, even in the absence of sevoflurane exposure, is sufficient to induce ACC hyperactivation, leading to impaired remote memory recall in presymptomatic AD mice.

Lastly, we investigated whether clinical medications used to control neuronal overexcitation could alleviate remote memory impairment induced by sevoflurane. Clonazepam, a benzodiazepine known to act as a $GABA_A$-receptor agonist and commonly used to treat insomnia and anxiety-related disorders, has shown promise in attenuating cognitive deficits in mouse models of AD by reducing neuronal hyperactivation.[56] To test whether clonazepam could rescue remote memory deficits induced by sevoflurane, we administered a low dose of clonazepam (0.05 mg/kg) intraperitoneally 30 min prior to in vivo Ca^{2+} imaging and the recall test (Figure 5G). We found that clonazepam treatment effectively reduced pyramidal neuron activity in the ACC of 5×FAD mice (Figure 5H), bringing it to levels comparable to those observed in mice without sevoflurane exposure. Furthermore, when we assessed spatial memory in the Barnes maze, we found that clonazepam treatment reversed the spatial memory deficit in 5×FAD mice subjected to sevoflurane anesthesia (Figure 5I). These results indicate that restoring neuronal activity in the CA1-ACC circuits can reverse the remote recall deficits induced by sevoflurane.

$U = 1253$, $p = .0909$). (C) Experimental design for imaging CA1→ACC axonal terminals in ACC. (D) Representative two-photon image (left), Ca^{2+} traces (middle), and quantification of axonal Ca^{2+} activity in 3-month-old 5×FAD mice with recent exposure to air or sevoflurane ($n = 109, 132$ axons from four mice per group, Mann–Whitney test, $U = 1017$, $p < .0001$). (E) Experimental design for in vivo Ca^{2+} imaging of CA1 neurons projecting to ACC. (F) Representative two-photon image (left), Ca^{2+} traces (middle), and quantification of somatic Ca^{2+} activity in CA1 neurons ($n = 338, 353$ cells from five mice per group, Mann–Whitney test, $U = 47715$, $p < .0001$). (G) Experimental design for selective expression of tdTomato in ACC neurons that receive direct projections from CA1. (H) Confocal image of tdTomato$^+$ neurons in ACC. (I) Distribution of tdTomato$^+$ neurons across layers in ACC. (J) Confocal images of ACC showing colocalization of tdTomato$^+$ neurons with different neuronal markers. (K) Percentages of tdTomato$^+$ neurons colocalized with glutamatergic or GABAergic neurons ($n = 3$ mice). Summary data are presented as mean ± SEM. Each dot represents data from a single cell (B, D, F) or animal (K).

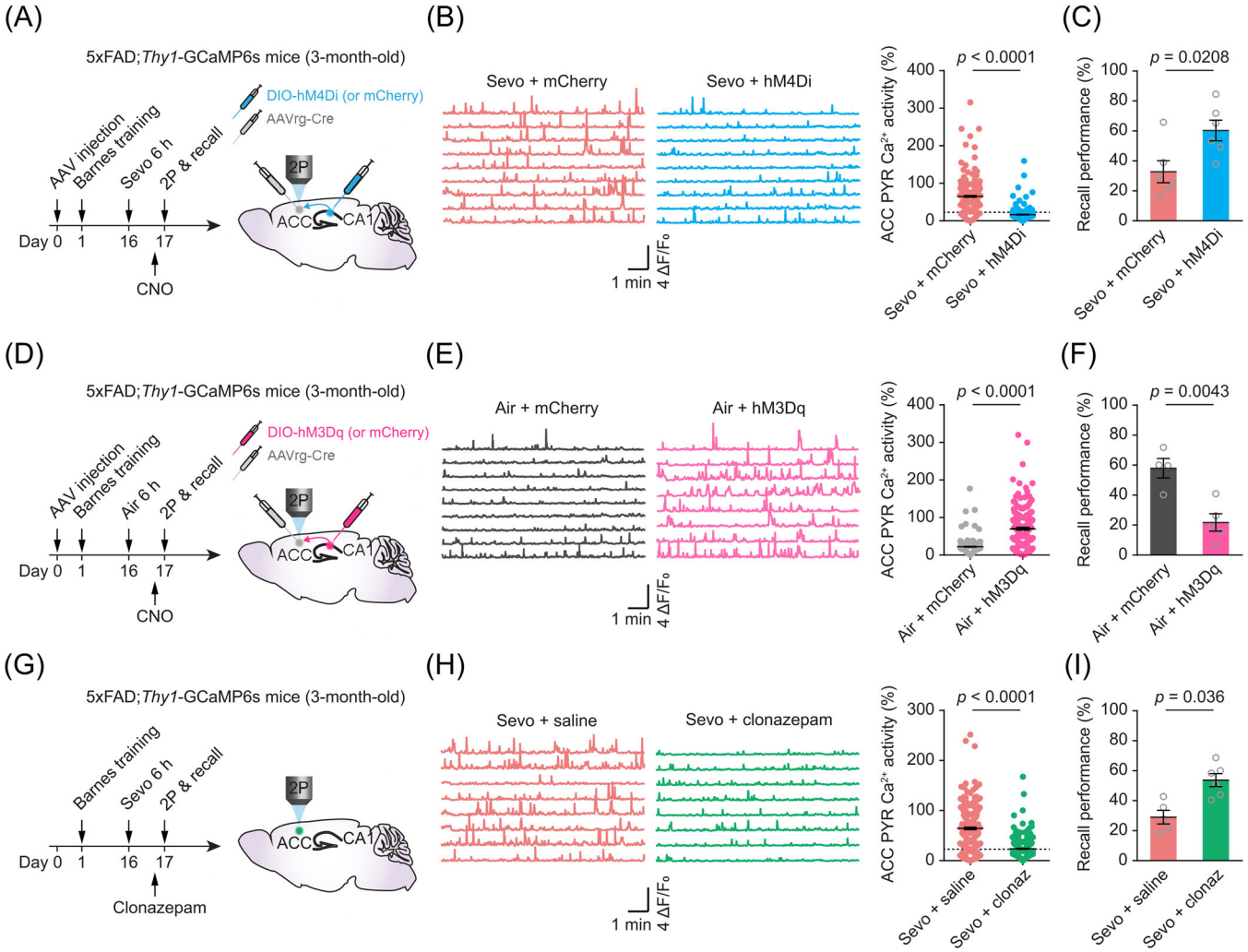

FIGURE 5 Inhibition of CA1-ACC hyperactivity protects against sevoflurane-induced remote memory impairment. (A) Experimental design and timeline for chemogenetic inhibition of CA1-ACC projection neurons in 3-month-old 5×FAD mice with recent exposure to sevoflurane. (B) Representative Ca^{2+} traces of ACC pyramidal neurons 30 min after CNO administration (left) and quantification of Ca^{2+} activity (right, $n = 269$, 220 cells from four mice per group, unpaired t test, $t_{487} = 17.79$, $p < .0001$). The dashed line indicates the Ca^{2+} level in 5×FAD mice with air exposure. (C) Recall performance in Barnes maze test ($n = 6$ mice per group, unpaired t test, $t_{10} = 2.74$, $p = .0208$). (D) Experimental design and timeline for chemogenetic activation of CA1-ACC projection neurons in 3-month-old 5×FAD mice without recent sevoflurane exposure. (E) Representative Ca^{2+} traces of ACC pyramidal neurons 30 min after CNO injection (left) and quantification of Ca^{2+} activity (right; $n = 219$, 251 cells from four mice per group, unpaired t test, $t_{468} = 17.79$, $p < .0001$). (F) Recall performance in Barnes maze ($n = 4$, 5 mice; unpaired t test, $t_7 = 4.15$, $p = .0043$). (G) Experimental design and timeline. Low-dose clonazepam, a $GABA_A$-receptor agonist, was administered 30 min before Ca^{2+} imaging and recall test in 5×FAD mice with recent exposure to sevoflurane. (H) Left, representative Ca^{2+} traces of ACC pyramidal neurons following saline or clonazepam injection. Right, quantification of ACC pyramidal neuron Ca^{2+} activity ($n = 266$, 251 cells from four mice per group, unpaired t test, $t_{515} = 14.81$, $p < .0001$). The dashed line indicates the Ca^{2+} level in 5×FAD mice with air exposure. (I) Recall performance in Barnes maze test ($n = 5$, 6 mice, unpaired t test, $t_9 = 3.908$, $p = .036$). Summary data are presented as mean ± SEM. Each dot represents data from a single cell (B, E, H) or animal (C, F, I).

3.6 | Tau hyperphosphorylation contributes to neural network dysfunction and remote memory impairment

How does sevoflurane induce ACC hyperactivation? Previous studies indicated that sevoflurane may increase tau phosphorylation in the brain,[22–26] and tau hyperphosphorylation has been associated with neuronal network hyperexcitability.[57] To test this possibility, we performed immunostaining of phospho-tau (p-tau) using the AT8 antibody in the CA1 and ACC of 5×FAD mice (Figure 6A). Our results showed that 5×FAD mice treated with sevoflurane exhibited a higher level of p-tau in the CA1 region than those treated with air (Figure 6B,C). There was no significant difference in the amount of p-tau in the ACC of 5×FAD mice following air or sevoflurane exposure (Figure S9).

Given the critical role of CA1 activation in driving ACC hyperactivity, we next tested whether inhibiting tau phosphorylation in the CA1 could prevent sevoflurane-induced neuronal hyperactivity and remote recall deficits. To this end, we performed a bilateral infusion of tau

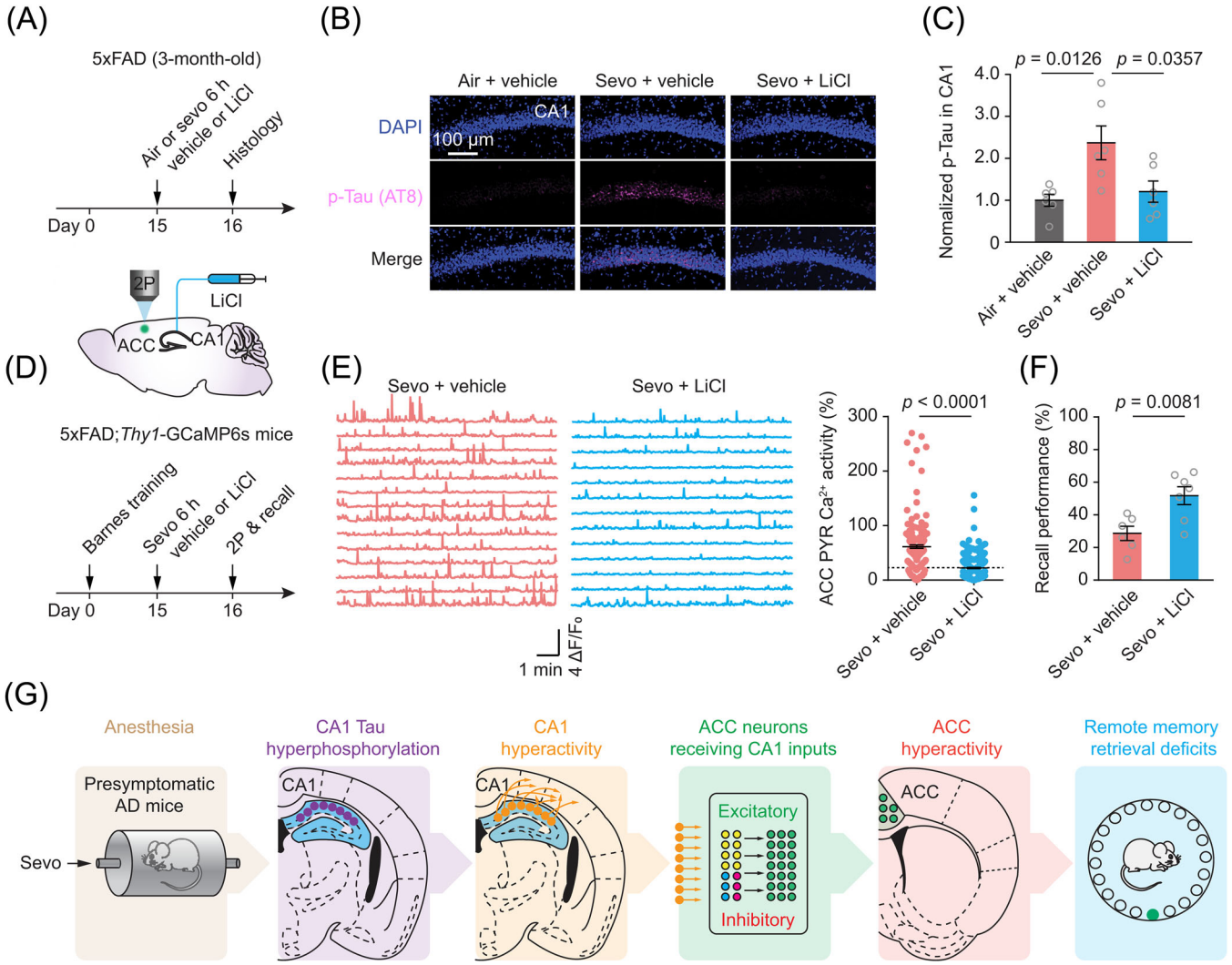

FIGURE 6 Hippocampal tau hyperphosphorylation contributes to ACC hyperactivity and remote memory impairment. (A) Experimental timeline. (B) Representative immunofluorescent images of hippocampal CA1 region showing p-tau (AT8) expression. (C) Exposure to sevoflurane increased the level of p-tau in the CA1 region of the hippocampus ($n = 6$ mice per group, one-way ANOVA, $F_{(2, 15)} = 1.752$, $p = .0088$; Air + vehicle vs Sevo + vehicle, $p = .0126$), which can be alleviated by the infusion of tau antagonist LiCl during anesthesia (Sevo + vehicle vs Sevo + LiCl, $p = .0357$). (D) Experimental design (top) and timeline (bottom) for Barnes training, sevoflurane exposure, LiCl infusion, and in vivo Ca^{2+} imaging in 5×FAD mice. (E) Representative Ca^{2+} traces (left) and average Ca^{2+} activity (right, $n = 198, 293$ cells from four mice per group, unpaired t test, $t_{489} = 13.75$, $p < .0001$) of ACC pyramidal neurons treated with vehicle or LiCl. The dashed line indicates the Ca^{2+} level in 5×FAD mice with air exposure. (F) Recall performance in Barnes maze test ($n = 6, 7$ mice per group, unpaired t test, $t_{11} = 3.226$, $p = .0081$). (G) Schematic summary. Hyperactivation of the CA1-ACC circuit, due to tau hyperphosphorylation in the hippocampus induced by sevoflurane, impedes remote memory retrieval in presymptomatic AD mouse models. Summary data are presented as mean ± SEM. Each dot represents data from a single cell (E) or animal (C, F).

inhibitor (LiCl, 100 mM) into the CA1 regions of 5×FAD mice during sevoflurane exposure (Figure 6D). The following day, mice treated with LiCl showed a significant reduction in the levels of p-tau in the CA1 compared to those treated with vehicle (Figure 6B,C). Moreover, Ca^{2+} activity in ACC pyramidal neurons was markedly decreased, reaching a level comparable to that observed in 5×FAD mice without sevoflurane exposure (Figure 6E). Behaviorally, sevoflurane-induced remote recall deficits in 5×FAD mice were also rescued (Figure 6F). These results indicate that suppressing tau hyperphosphorylation in the hippocampus can effectively prevent sevoflurane-induced ACC hyperactivation and remote recall deficits in presymptomatic AD mice (Figure 6G).

4 | DISCUSSION

Individuals with underlying AD pathology are susceptible to memory impairment following anesthesia and surgery.[1,2] However, the specific mechanisms by which anesthesia affects neuronal circuits, leading to remote memory impairment, are poorly understood. In this study,

we provide evidence that sevoflurane anesthesia induces increased tau phosphorylation in the hippocampus, which subsequently leads to hyperactivation of CA1-ACC circuits. These effects ultimately disrupt the retrieval of remote memories in presymptomatic AD mouse models.

The ACC has been shown to be crucial for the storage and retrieval of remote spatial memory.[16] Our findings reveal that prolonged sevoflurane anesthesia induces abnormal hyperactivation of pyramidal neurons in the ACC of 3-month-old 5×FAD mice and 5-month-old APP/PS1 mice, both of which are in the presymptomatic phases of AD. This hyperactivation of ACC pyramidal neurons is strongly associated with the animals' remote recall impairment in the Barnes maze test. Moreover, we observed alterations in the activity of local inhibitory interneurons in the ACC following anesthesia. Specifically, there was a trend of decreased activity in inhibitory PV interneurons, while disinhibitory VIP interneurons exhibited increased activity. Both of these changes favor heightened pyramidal neuron activity. These findings align with previous reports of increased pyramidal neuron activity in the prefrontal cortex of aged mice during emergence from sevoflurane anesthesia.[27] Additionally, other research groups have reported enhanced pyramidal neuronal activity following isoflurane anesthesia, which involves modulation of GABAergic boutons of PV interneurons.[58] Moreover, repeated anesthesia has been linked to reduced PV neuronal activity and the loss of PV interneurons.[59,60]

In this study, we did not observe significant changes in SST and CRH interneuron activity 24 h after sevoflurane anesthesia. Among GABAergic neurons in the prefrontal cortex, CRH neurons constitute a significant proportion and have been implicated in the modulation of affective behaviors such as anxiety and social withdrawal.[47,48] Our findings of unaltered CRH neuronal activity are consistent with the observation that 5×FAD mice did not exhibit anxiety-like behavior following sevoflurane exposure. Nonetheless, it is important to note that a significant number of patients undergoing major surgery involving anesthesia have reported symptoms of depression and anxiety.[61] Future studies are needed to explore the potential impact of anesthesia in combination with surgery on CRH neuron function and its potential association with postsurgical affective disorders.

Anesthesia-induced hyperactivation of the ACC is primarily driven by increased excitatory inputs from the hippocampal CA1. Using viral-based circuit tracing techniques, we identified that most excitatory inputs projecting to the ACC originate from the CA1 and MDT. Despite the known influence of general anesthesia on the thalamus,[51] we did not observe significant changes in MDT-ACC axonal activity 24 h after sevoflurane exposure. In contrast, we observed a notable increase in CA1-ACC axonal activity within the ACC. In vivo Ca^{2+} imaging in the CA1 region revealed heightened somatic activity of neurons projecting to the ACC, suggesting that abnormal hippocampal activity may contribute to the hyperactivation of ACC. This observation is particularly noteworthy considering the susceptibility of the hippocampus to the effects of anesthetics and AD pathologies.[54] To test this hypothesis, we selectively inhibited the excitatory inputs from CA1 to ACC using inhibitory DREADD and found that this intervention normalized neuronal activity in the ACC and improved the retrieval of remote memories in 5×FAD mice.

Previous studies have demonstrated functional connections between the hippocampus and prefrontal circuits. In vitro and in vivo electrophysiological recordings have shown that both excitatory and inhibitory neurons in the prefrontal cortex exhibit postsynaptic currents upon stimulation of the hippocampus.[62–64] In this study, we employed anterograde tracing and post hoc immunofluorescent staining techniques to investigate the connectivity between the ACC and CA1 neurons. Our findings indicate that both glutamatergic and GABAergic neurons in the ACC form monosynaptic connections with CA1 neurons. However, previous studies examining projections from the ACC to the hippocampus produced varied results. Some studies identified monosynaptic connections from ACC pyramidal neurons to hippocampal pyramidal cells in the CA3/CA1 regions[65] or from prefrontal GABAergic neurons to hippocampal disinhibitory interneurons[66] using retrograde tracing and anterograde electrophysiological recording methods. In contrast, a recent study did not find evidence of direct, monosynaptic projection from the ACC to the hippocampus.[67]

Our findings, obtained from mouse models of AD, provide support for the standard consolidation theory, which proposes that the hippocampus plays a critical role in encoding contextual memory under normal physiological conditions. Once acquired, remote memory becomes less dependent on the hippocampus and is distributed more broadly across neocortical circuits.[12] However, our results also indicate that disruptions in the connectivity between the hippocampus and cortical circuits can still impact the retrieval of remote memories. Importantly, we found that the majority of GABAergic neurons in the ACC that receive direct inputs from the hippocampus are VIP interneurons. Inhibiting VIP interneurons in the ACC prevents sevoflurane-induced deficits in remote recall in presymptomatic AD mice. These findings suggest a crucial role of VIP cells in modulating CA1-ACC circuits and facilitating the retrieval of previously acquired spatial memories. Additionally, consistent with previous reports,[56] we found that systemic administration of low-dose clonazepam can restore normal CA1-ACC network function and protect remote memory in AD mice.

An important finding of the current study is that tau hyperphosphorylation may serve as a potential mechanism underlying sevoflurane-induced neural network hyperactivity and remote memory impairment. This finding aligns with previous observations in older adults, in which higher tau levels have been correlated with hippocampal hyperactivity,[30] and a reduction of hippocampal hyperactivity has been shown to improve cognition.[68] Neuronal hyperexcitability is recognized as an early functional hallmark of AD. Recent studies have revealed early abnormal neuronal activity in the hippocampal and cortical regions of AD patients and animal models.[69–71] Furthermore, prior research has demonstrated that hyperphosphorylated tau contributes to neuronal network hyperexcitability,[57] and inhibition of tau hyperphosphorylation in the brain restores normal neuronal network activity.[72,73] Our immunofluorescent staining data revealed the presence of tau hyperphosphorylation specifically in the hippocampal CA1

region following sevoflurane anesthesia, while no tau hyperphosphorylation was observed in the ACC. Consistently, we found that inhibition of CA1 tau phosphorylation through LiCl infusion prevented the hyperactivity of ACC pyramidal neurons and rescued the impairment of remote memory. These findings highlight the therapeutic potential of tau inhibitors for the treatment of retrograde amnesia.

This study has several limitations. First, the mice in our study underwent surgical procedures, including cranial window implantation and viral injection, which involved the use of a different anesthetic, prior to the Barnes maze testing and subsequent imaging. These additional variables have the potential to influence the behavior and neuronal activity of the animals. Although our previous study demonstrated that brief anesthesia and surgical preparation did not have long-lasting effects on neural plasticity and learning ability in adult WT mice,[74,75] future studies should investigate whether these factors could affect 5×FAD mice differently. Second, our study focused solely on exploring tau hyperphosphorylation as a potential mechanism underlying anesthesia-induced remote memory impairment in 5×FAD mice. Since 5×FAD is a model of amyloidopathy, further investigations examining amyloid pathology will be necessary to obtain a more comprehensive understanding of the mechanisms underpinning anesthesia-induced neural circuit dysfunction. Third, caution must be exercised when extrapolating the clinical relevance of our findings in mouse models, as it is challenging to perform equivalent physiological monitoring during anesthesia in mice as conducted in human patients, which limits the direct translation of our results to the clinical setting. It is important to note that while our study and some other animal studies suggest an association between exposure to anesthesia and the development or exacerbation of learning and memory impairment,[5] there is currently no direct evidence supporting a causal link between anesthesia exposure and AD in humans.

5 | CONCLUSION

In summary, our study in presymptomatic AD mouse models indicates that remote memory impairment induced by anesthesia may arise from the hyperactivation of CA1-ACC circuits. Moreover, we identify tau hyperphosphorylation as a potential therapeutic target for preserving neural network function in AD. Further investigations using other AD models, such as apolipoprotein E4 (*APOE4*), could provide additional insights into the involvement of neuronal network hyperactivity in memory impairment associated with AD.

AUTHOR CONTRIBUTIONS

Kai Chen initiated this project. Kai Chen, Meng Cui, Zhongcong Xie, and Guang Yang designed the research study. Kai Chen performed most of the experiments. Riya Gupta performed behavioral and immunostaining experiments. Alejandro Martín-Ávila provided mouse resources. Kai Chen and Riya Gupta analyzed data with input from Meng Cui, Zhongcong Xie, and Guang Yang. Kai Chen and Guang Yang wrote the paper. All authors reviewed and revised the manuscript.

ACKNOWLEDGMENTS

The authors thank Viola Neudecker and Jose Perez-Zoghbi for their assistance with blood gas measurements and Yang lab members for the helpful discussions. This research was supported by National Institutes of Health GM131765 (to G.Y.), AG041274 and AG062509 (to Z.X.), and NS118302 (to M.C.). A. M-A. was supported by Alzheimer's Association AARFD-17-533584.

CONFLICT OF INTEREST STATEMENT

Dr. Zhongcong Xie provided consulting services to Shanghai 9th and 10th Hospitals, Baxter (invited speaker), NanoMosaic and the *Journal of Anesthesiology and Perioperative Science* in the last 36 months. All the authors declare no competing interests in the present study. Author disclosures are available in the supporting information. Author disclosures are available in the supporting information.

CONSENT STATEMENT

This study did not involve any human subjects. Consent was not necessary.

REFERENCES

1. Berger M, Burke J, Eckenhoff R, Mathew J. Alzheimer's disease, anesthesia, and surgery: a clinically focused review. *J Cardiothorac Vasc Anesth*. 2014;28(6):1609-1623.
2. Vutskits L, Xie Z. Lasting impact of general anaesthesia on the brain: mechanisms and relevance. *Nat Rev Neurosci*. 2016;17(11):705-717.
3. Walker KA, Le Page LM, Terrando N, Duggan MR, Heneka MT, Bettcher BM. The role of peripheral inflammatory insults in Alzheimer's disease: a review and research roadmap. *Mol Neurodegener*. 2023;18(1):37.
4. Fong TG, Inouye SK. The inter-relationship between delirium and dementia: the importance of delirium prevention. *Nat Rev Neurol*. 2022;18(10):579-596.
5. Eckenhoff RG, Maze M, Xie Z, et al. Perioperative neurocognitive disorder: state of the preclinical science. *Anesthesiology*. 2020;132(1):55-68.
6. Bianchi SL, Tran T, Liu C, et al. Brain and behavior changes in 12-month-old Tg2576 and nontransgenic mice exposed to anesthetics. *Neurobiol Aging*. 2008;29(7):1002-1010.
7. Planel E, Bretteville A, Liu L, et al. Acceleration and persistence of neurofibrillary pathology in a mouse model of tauopathy following anesthesia. *FASEB J*. 2009;23(8):2595-2604.
8. Tian D, Xing Y, Gao W, et al. Sevoflurane aggravates the progress of Alzheimer's disease through NLRP3/Caspase-1/Gasdermin D Pathway. *Front Cell Dev Biol*. 2021;9:801422.
9. Eichenbaum H. Prefrontal-hippocampal interactions in episodic memory. *Nat Rev Neurosci*. 2017;18(9):547-558.
10. Burgess N, Maguire EA, O'Keefe J. The human hippocampus and spatial and episodic memory. *Neuron*. 2002;35(4):625-641.
11. Bannerman DM, Sprengel R, Sanderson DJ, et al. Hippocampal synaptic plasticity, spatial memory and anxiety. *Nat Rev Neurosci*. 2014;15(3):181-192.
12. Frankland PW, Bontempi B. The organization of recent and remote memories. *Nat Rev Neurosci*. 2005;6(2):119-130.
13. Bontempi B, Laurent-Demir C, Destrade C, Jaffard R. Time-dependent reorganization of brain circuitry underlying long-term memory storage. *Nature*. 1999;400(6745):671-675.
14. Maviel T, Durkin TP, Menzaghi F, Bontempi B. Sites of neocortical reorganization critical for remote spatial memory. *Science*. 2004;305(5680):96-99.

15. Takehara-Nishiuchi K, McNaughton BL. Spontaneous changes of neocortical code for associative memory during consolidation. *Science*. 2008;322(5903):960-963.
16. Teixeira CM, Pomedli SR, Maei HR, Kee N, Frankland PW. Involvement of the anterior cingulate cortex in the expression of remote spatial memory. *J Neurosci*. 2006;26(29):7555-7564.
17. Goshen I, Brodsky M, Prakash R, et al. Dynamics of retrieval strategies for remote memories. *Cell*. 2011;147(3):678-689.
18. Holtzman DM, Carrillo MC, Hendrix JA, et al. Tau: from research to clinical development. *Alzheimers Dement*. 2016;12(10):1033-1039.
19. Iqbal K, Liu F, Gong CX. Grundke-Iqbal I. Tau in Alzheimer disease and related tauopathies. *Current Alzheimer Research*. 2010;7(8):656-664.
20. Wang Y, Mandelkow E. Tau in physiology and pathology. *Nat Rev Neurosci*. 2016;17(1):5-21.
21. Whittington RA, Bretteville A, Dickler MF. Planel E. Anesthesia and tau pathology. *Prog Neuropsychopharmacol Biol Psychiatry*. 2013;47:147-155.
22. Le Freche H, Brouillette J, Fernandez-Gomez FJ, et al. Tau phosphorylation and sevoflurane anesthesia: an association to postoperative cognitive impairment. *Anesthesiology*. 2012;116(4):779-787.
23. Tao G, Zhang J, Zhang L, et al. Sevoflurane induces tau phosphorylation and glycogen synthase kinase 3beta activation in young mice. *Anesthesiology*. 2014;121(3):510-527.
24. Yu Y, Yang Y, Tan H, et al. Tau contributes to sevoflurane-induced neurocognitive impairment in neonatal mice. *Anesthesiology*. 2020;133(3):595-610.
25. Yang Y, Liang F, Gao J, et al. Testosterone attenuates sevoflurane-induced tau phosphorylation and cognitive impairment in neonatal male mice. *Br J Anaesth*. 2021;127(6):929-941.
26. Dong Y, Liang F, Huang L, et al. The anesthetic sevoflurane induces tau trafficking from neurons to microglia. *Commun Biol*. 2021;4(1):560.
27. Chen K, Hu Q, Gupta R, Stephens J, Xie Z, Yang G. Inhibition of unfolded protein response prevents post-anesthesia neuronal hyperactivity and synapse loss in aged mice. *Aging Cell*. 2022;21(4):e13592.
28. Ballweg T, White M, Parker M, et al. Association between plasma tau and postoperative delirium incidence and severity: a prospective observational study. *Br J Anaesth*. 2021;126(2):458-466.
29. Liang F, Baldyga K, Quan Q, et al. Preoperative plasma Tau-PT217 and Tau-PT181 are associated with postoperative delirium. *Ann Surg*. 2022.
30. Berron D, Cardenas-Blanco A, Bittner D, et al. Higher CSF tau levels are related to hippocampal hyperactivity and object mnemonic discrimination in older adults. *J Neurosci*. 2019;39(44):8788.
31. Huijbers W, Schultz AP, Papp KV, et al. Tau accumulation in clinically normal older adults is associated with hippocampal hyperactivity. *J Neurosci*. 2019;39(3):548.
32. Cichon J, Magrane J, Shtridler E, et al. Imaging neuronal activity in the central and peripheral nervous systems using new Thy1.2-GCaMP6 transgenic mouse lines. *J Neurosci Methods*. 2020;334:108535.
33. Phan K, Kim JS, Kim JH, et al. Anesthesia duration as an independent risk factor for early postoperative complications in adults undergoing elective ACDF. *Global Spine J*. 2017;7(8):727-734.
34. Satomoto M, Satoh Y, Terui K, et al. Neonatal exposure to sevoflurane induces abnormal social behaviors and deficits in fear conditioning in mice. *Anesthesiology*. 2009;110(3):628-637.
35. Planel E, Richter KE, Nolan CE, et al. Anesthesia leads to tau hyperphosphorylation through inhibition of phosphatase activity by hypothermia. *J Neurosci*. 2007;27(12):3090-3097.
36. Hector A, McAnulty C, Piche-Lemieux ME, et al. Tau hyperphosphorylation induced by the anesthetic agent ketamine/xylazine involved the calmodulin-dependent protein kinase II. *FASEB J*. 2020;34(2):2968-2977.
37. Sun M, Dong Y, Li M, et al. Dexmedetomidine and clonidine attenuate sevoflurane-induced tau phosphorylation and cognitive impairment in young mice via alpha-2 adrenergic receptor. *Anesth Analg*. 2021;132(3):878-889.
38. Attar A, Liu T, Chan W-TC, et al. A shortened barnes maze protocol reveals memory deficits at 4-months of age in the triple-transgenic mouse model of Alzheimer's disease. *PLoS One*. 2013;8(11):e80355.
39. Hong M, Chen DC, Klein PS, Lee VM. Lithium reduces tau phosphorylation by inhibition of glycogen synthase kinase-3. *J Biol Chem*. 1997;272(40):25326-25332.
40. Chen K, Hu Q, Xie Z, Yang G. Monocyte NLRP3-IL-1β hyperactivation mediates neuronal and synaptic dysfunction in perioperative neurocognitive disorder. *Adv Sci*. 2022;n/a(n/a):2104106.
41. Ulivi AF, Castello-Waldow TP, Weston G, et al. Longitudinal two-photon imaging of dorsal hippocampal CA1 in live mice. *J Vis Exp*. 2019(148).
42. Wei B, Wang C, Cheng Z, Lai B, Gan WB, Cui M. Clear optically matched panoramic access channel technique (COMPACT) for large-volume deep brain imaging. *Nat Methods*. 2021;18(8):959-964.
43. Chen K, Yang G, So KF, Zhang L. Activation of cortical somatostatin interneurons rescues synapse loss and motor deficits after acute MPTP infusion. *iScience*. 2019;17:230-241.
44. Huang L, Cichon J, Ninan I, Yang G. Post-anesthesia AMPA receptor potentiation prevents anesthesia-induced learning and synaptic deficits. *Sci Transl Med*. 2016;8(344):344ra385.
45. Lu J, Liang F, Bai P, et al. Blood tau-PT217 contributes to the anesthesia/surgery-induced delirium-like behavior in aged mice. *Alzheimers Dement*. 2023.
46. Urban DJ, Roth BL. DREADDs (designer receptors exclusively activated by designer drugs): chemogenetic tools with therapeutic utility. *Annu Rev Pharmacol Toxicol*. 2015;55:399-417.
47. Risbrough VB, Stein MB. Role of corticotropin releasing factor in anxiety disorders: a translational research perspective. *Horm Behav*. 2006;50(4):550-561.
48. Dedic N, Kuhne C, Gomes KS, et al. Deletion of CRH from GABAergic forebrain neurons promotes stress resilience and dampens stress-induced changes in neuronal activity. *Front Neurosci*. 2019;13:986.
49. Tremblay R, Lee S, Rudy B. GABAergic interneurons in the neocortex: from cellular properties to circuits. *Neuron*. 2016;91(2):260-292.
50. Bush G, Luu P, Posner MI. Cognitive and emotional influences in anterior cingulate cortex. *Trends Cogn Sci*. 2000;4(6):215-222.
51. Hudetz AG. General anesthesia and human brain connectivity. *Brain Connectivity*. 2012;2(6):291-302.
52. Broussard GJ, Liang Y, Fridman M, et al. In vivo measurement of afferent activity with axon-specific calcium imaging. *Nat Neurosci*. 2018;21(9):1272-1280.
53. Meda KS, Patel T, Braz JM, et al. Microcircuit mechanisms through which mediodorsal thalamic input to anterior cingulate cortex exacerbates pain-related aversion. *Neuron*. 2019;102(5):944-959. e943.
54. DeTure MA, Dickson DW. The neuropathological diagnosis of Alzheimer's disease. *Mol Neurodegener*. 2019;14(1):32.
55. Zingg B, Chou X-l, Zhang Z-g, et al. AAV-mediated anterograde transsynaptic tagging: mapping corticocollicular input-defined neural pathways for defense behaviors. *Neuron*. 2017;93(1):33-47.
56. Busche MA, Kekus M, Adelsberger H, et al. Rescue of long-range circuit dysfunction in Alzheimer's disease models. *Nat Neurosci*. 2015;18(11):1623-1630.
57. Kazim SF, Seo JH, Bianchi R, et al. Neuronal network excitability in Alzheimer's disease: the puzzle of similar versus divergent roles of amyloid beta and tau. *eNeuro*. 2021;8(2). ENEURO.0418-0420.2020.
58. Haruwaka K, Ying Y, Liang Y, et al. Microglial process dynamics enhance neuronal activity by shielding GABAergic synaptic inputs. *Biorxiv*. 2022. 2022.2011.2008.515728.
59. Roque PS, Thorn Perez C, Hooshmandi M, et al. Parvalbumin interneuron loss mediates repeated anesthesia-induced memory deficits in mice. *J Clin Invest*. 2023;133(2).
60. Zhou H, Xie Z, Brambrink AM, Yang G. Behavioural impairments after exposure of neonatal mice to propofol are accompanied by

reductions in neuronal activity in cortical circuitry. *Br J Anaesth*. 2021;126(6):1141-1156.
61. Ghoneim MM, O'Hara MW. Depression and postoperative complications: an overview. *BMC Surg*. 2016;16(1):5.
62. Tierney PL, Degenetais E, Thierry AM, Glowinski J, Gioanni Y. Influence of the hippocampus on interneurons of the rat prefrontal cortex. *Eur J Neurosci*. 2004;20(2):514-524.
63. Parent MA, Wang L, Su J, Netoff T, Yuan L-L. Identification of the hippocampal input to medial prefrontal cortex in vitro. *Cereb Cortex*. 2010;20(2):393-403.
64. Wang DV, Ikemoto S. Coordinated interaction between hippocampal sharp-wave ripples and anterior cingulate unit activity. *J Neurosci*. 2016;36(41):10663.
65. Rajasethupathy P, Sankaran S, Marshel JH, et al. Projections from neocortex mediate top-down control of memory retrieval. *Nature*. 2015;526(7575):653-659.
66. Malik R, Li Y, Schamiloglu S, Sohal VS. Top-down control of hippocampal signal-to-noise by prefrontal long-range inhibition. *Cell*. 2022;185(9):1602-1617. e1617.
67. Andrianova L, Yanakieva S, Margetts-Smith G, et al. No evidence from complementary data sources of a direct projection from the mouse anterior cingulate cortex to the hippocampal formation. *Biorxiv*. 2022. 2022.2001.2025.477805.
68. Bakker A, Krauss GL, Albert MS, et al. Reduction of hippocampal hyperactivity improves cognition in amnestic mild cognitive impairment. *Neuron*. 2012;74(3):467-474.
69. Minkeviciene R, Rheims S, Dobszay MB, et al. Amyloid beta-induced neuronal hyperexcitability triggers progressive epilepsy. *J Neurosci*. 2009;29(11):3453-3462.
70. Quiroz YT, Budson AE, Celone K, et al. Hippocampal hyperactivation in presymptomatic familial Alzheimer's disease. *Ann Neurol*. 2010;68(6):865-875.
71. Busche MA, Chen X, Henning HA, et al. Critical role of soluble amyloid-beta for early hippocampal hyperactivity in a mouse model of Alzheimer's disease. *Proc Natl Acad Sci USA*. 2012;109(22):8740-8745.
72. Chang C-W, Evans MD, Yu X, Yu G-Q, Mucke L. Tau reduction affects excitatory and inhibitory neurons differently, reduces excitation/inhibition ratios, and counteracts network hypersynchrony. *Cell Rep*. 2021;37(3):109855.
73. Holth JK, Bomben VC, Reed JG, et al. Tau loss attenuates neuronal network hyperexcitability in mouse and Drosophila Genetic Models of Epilepsy. *J Neurosci*. 2013;33(4):1651.
74. Huang L, Yang G. Repeated exposure to ketamine-xylazine during early development impairs motor learning-dependent dendritic spine plasticity in adulthood. *Anesthesiology*. 2015;122(4):821-831.
75. Yang G, Chang PC, Bekker A, Blanck TJ, Gan WB. Transient effects of anesthetics on dendritic spines and filopodia in the living mouse cortex. *Anesthesiology*. 2011;115(4):718-726.

SUPPORTING INFORMATION

Additional supporting information can be found online in the Supporting Information section at the end of this article.

How to cite this article: Chen K, Gupta R, Martín-Ávila A, Cui M, Xie Z, Yang G. Anesthesia-induced hippocampal-cortical hyperactivity and tau hyperphosphorylation impair remote memory retrieval in Alzheimer's disease. *Alzheimer's Dement*. 2024;20:494–510. https://doi.org/10.1002/alz.13464